Molecular Cancer Therapeutics

Efficient Gene Silencing in Brain Tumors with Hydrophobically Modified siRNAs

Maire F. Osborn[1,2], Andrew H. Coles[1,2], Diane Golebiowski[3,4], Dimas Echeverria[1,2], Michael P. Moazami[1,5], Jonathan K. Watts[1,5], Miguel Sena-Esteves[3,4], and Anastasia Khvorova[1,2]

Abstract

Glioblastoma (GBM) is the most common and lethal form of primary brain tumor with dismal median and 2-year survivals of 14.5 months and 18%, respectively. The paucity of new therapeutic agents stems from the complex biology of a highly adaptable tumor that uses multiple survival and proliferation mechanisms to circumvent current treatment approaches. Here, we investigated the potency of a new generation of siRNAs to silence gene expression in orthotopic brain tumors generated by transplantation of human glioma stem-like cells in athymic nude mice. We demonstrate that cholesterol-conjugated, nuclease-resistant siRNAs (Chol-hsiRNAs) decrease mRNA and silence luciferase expression by 90% *in vitro* in GBM neurospheres. Furthermore, Chol-hsiRNAs distribute broadly in brain tumors after a single intratumoral injection, achieving sustained and potent (>45% mRNA and >90% protein) tumor-specific gene silencing. This readily available platform is sequence-independent and can be adapted to target one or more candidate GBM driver genes, providing a straightforward means of modulating GBM biology *in vivo*. *Mol Cancer Ther; 17(6); 1251–8. ©2018 AACR.*

Introduction

Glioblastoma (GBM, or grade IV astrocytoma) is the most frequent and lethal primary malignant brain tumor in humans, characterized by invasiveness, angiogenesis, and frequent necrosis (1). Current treatments are limited to surgical tumor resection, followed by chemotherapy with temozolomide and radiotherapy, and do not greatly improve prognosis (2, 3). GBM recurrence is almost inevitable, due in part to stem-like tumor cells [glioma stem-like cells (GSC) or tumor-initiating cells] that are both highly invasive and resistant to chemotherapy and radiotherapy (4). These challenges underscore the need for novel approaches to GBM treatment.

The massive repository of information available from cancer genomics studies and the ever-expanding knowledge about the role of GSCs in tumor biology have revealed a large number of genes and networks that orchestrate many of the pernicious properties of GBM (5–7). However, small-molecule drugs, which have been the mainstay of the pharmaceutical industry, can only target 10% to 15% of proteins encoded in the genome, and primarily those with enzymatic activity (8). A considerable number of genes (e.g., transcription factors, histones, extracellular matrix proteins), long noncoding RNAs (lncRNA), and miRNAs critical to GBM biology are not targetable by this approach. In contrast, siRNAs and antisense oligonucleotides can target any coding (mRNA) or noncoding RNA (lncRNA or miRNA; ref. 9). Therapeutic oligonucleotides are a highly flexible platform because target specificity is defined by the base sequence and can to some extent be optimized independently from the Pharmacokinetics/pharmacodynamics (PK/PD) properties (defined by the backbone chemistry and targeting ligand); this separation does not exist for small-molecule drugs, where the structure determines both properties (9). Therefore, oligonucleotide therapeutics have the necessary combination of specificity and flexibility to develop potent network (multi-mechanistic) drugs to effectively control GBM tumors (10).

Here, we investigated the activity of a next-generation siRNA (cholesterol-conjugated hsiRNA, Chol-hsiRNA; ref. 11) in GBM8 cells, a patient-derived tumor-initiating GSC line (12). Chol-hsiRNAs are asymmetric siRNAs with a short duplex region (15 base pairs) and a single-stranded, fully phosphorothioate-modified tail (13). The 2′-hydroxyl group in each nucleotide is substituted with 2′-fluoro or 2′-O-methyl modifications in an alternating pattern to provide stability and block innate immune activation (11, 14–16). The 3′ end of the passenger strand is conjugated to cholesterol to enhance cellular uptake (11). Previously, we have shown that Chol-hsiRNAs are rapidly internalized

[1]RNA Therapeutics Institute, University of Massachusetts Medical School, Worcester, Massachusetts. [2]Program in Molecular Medicine, University of Massachusetts Medical School, Worcester, Massachusetts. [3]Department of Neurology, University of Massachusetts Medical School, Worcester, Massachusetts. [4]Horae Gene Therapy Center, University of Massachusetts Medical School, Worcester, Massachusetts. [5]Department of Biochemistry and Molecular Pharmacology, University of Massachusetts Medical School, Worcester, Massachusetts.

Note: Supplementary data for this article are available at Molecular Cancer Therapeutics Online (http://mct.aacrjournals.org/).

M.F. Osborn and A.H. Coles contributed equally to this article.

Current address for D. Golebiowski: Solid GT, Cambridge, MA.

Corresponding Authors: Anastasia Khvorova, University of Massachusetts Medical School, 368 Plantation Street, Worcester, MA 01605. Phone: 774-455-3638; E-mail: Anastasia.Khvorova@umassmed.edu; or Miguel Sena-Esteves, Phone: 508-856-4412; Fax: 508-856-6696; E-mail: Miguel.Esteves@umassmed.edu

doi: 10.1158/1535-7163.MCT-17-1144

by neural cells both *in vitro* and *in vivo* and induce potent gene silencing in a carrier-free manner (11). Here, we show that Chol-hsiRNAs are also rapidly internalized into GBM8 cells and induce potent mRNA and protein silencing both *in vitro* and *in vivo* in established orthotopic brain tumors. Chol-hsiRNAs are informational drugs that can be used to target any sequence and thus can effectively manipulate gene expression in GBM, supporting the development of powerful new research tools and therapeutics for these devastating tumors.

Materials and Methods

Oligonucleotide synthesis

Oligonucleotides were synthesized on an Expedite ABI DNA/RNA Synthesizer following standard protocols. Each synthesis was done on a 1 μmole scale using cholesterol-conjugated CPG for the sense strand and Unylinker solid support (ChemGenes) for the antisense strand. All phosphoramidites [2′-O-methyl (ChemGenes), 2′-fluoro (BioAutomation), and Cy3 (Quasar570; Gene Pharma)] were prepared as 0.15 mol/L in acetonitrile (ACN). Phosphoramidite coupling time was 4 minutes using 30 equiv. of the monomer. 5-(Ethylthio)-1H-tetrazole (ETT) 0.25 mol/L in ACN was used as coupling activator. Detritylations were performed using 3% dichloroacetic acid in dichloromethane for 80 seconds, capping was done with acetic anhydride/THF/2,6-Lutidine, (80/10/10, v/v/v) (CAP A), and 1-methylimidazole/THF (16/84, v/v) (CAP B) for 15 seconds, and oxidation was achieved with 0.02 mol/L iodine in THF/pyridine/water (70/20/10, v/v/v) for 80 seconds. Phosphorothioate linkages were introduced using 0.1 mol/L solution of DDTT in ACN for 3 minutes.

Oligonucleotide deprotection and purification

Both sense and antisense strands were cleaved and deprotected using 1 mL of 40% aq. methylamine at 65°C for 15 minutes. The crude oligonucleotides were cooled, frozen in dry ice, and dried in a speedvac overnight. The resulting pellets were resuspended in 1 mL of 5% ACN. Antisense strand purification was performed on an Agilent 1100 series system equipped with an Agilent PL-SAX, a polymer ion exchange column (4.6 × 150 mm), using the following conditions: Eluent A: 30% ACN and Eluent B: 1 mol/L sodium perchlorate in 30% ACN, gradient: 0% B for 2 minutes, 0% to 10% B for 1 minute, 35% B for 8 minutes, equilibration to initial conditions for 6 minutes. Sense strand purification was performed on an Agilent 1100 series system equipped with a PRP-C18, a polymer reverse phase column (4.6 × 150 mm), using the following conditions: Eluent A: 50 mmol/L sodium acetate in 5% ACN and Eluent B: ACN, gradient: 0% B for 2 min, 0% to 40% B for 1 minute, 40% to 70% B for 8 minutes, equilibration to initial conditions for 6 minutes. Temperature was held at 70°C and flow rate at 10 mL/min for both cases. Peaks were monitored at 260 nm. Purified oligonucleotides were collected, frozen in dry ice, and dried in a speedvac overnight. Oligonucleotides were resuspended in 5% ACN, desalted through fine Sephadex G-25 columns built in house, lyophilized, and stored at −80°C until further use.

LC-MS analysis of oligonucleotides

The identity of oligonucleotides was established by LC-MS analysis on an Agilent 6530 accurate mass Q-TOF LC/MS machine using the following conditions: Buffer A: 100 mmol/L HFIP/9 mmol/L TEA in LC/MS grade water, Buffer B: 100 mmol/L HFIP/9 mmol/L TEA in LC/MS grade methanol, column: Agilent AdvanceBio oligonucleotides C18, gradient antisense: 0% B for 1 minute, 0% to 30% B for 8 minutes, equilibration for 4 minutes, gradient sense: 0% B for 1 minute, 0% to 50% B for 0.5 minute, 50% to 100% B for 8 minutes, equilibration for 4 minutes, temperature: 45°C, flow rate: 0.5 mL/min, UV (260 nm). MS parameters were as follows: Source: ESI, ion polarity: negative mode, range: 100 to 3,200 m/z, scan rate: 2 spectra/s, VCap: 4000, fragmentor: 180 V.

Cell culture

GBM8 primary human GBM cells were received as frozen stocks in 2014 from Dr. Miguel Sena-Esteves (University of Massachusetts Medical School), who originally obtained them from Dr. Samuel Rabkin (Massachusetts General Hospital, Boston, MA; ref. 12). Cells were certified mycoplasma negative by regular testing (MycoAlert, Lonza), with the last date of testing conducted 2 weeks prior to the first *in vitro* experiment. Cell authentication was not performed prior to conducting the experiments described in this article. The GBM8-fLuc cells used in these studies (17) were grown in suspension in Neurobasal media (Gibco) supplemented with 3 mmol/L L-Glutamine (CellGro), 1X B27 supplement (Gibco), 0.5X N2 supplement (Gibco), 2 μg/mL heparin (Sigma), 0.5X antibiotic–antimycotic solution (CellGro), 0.5X amphotericine B (CellGro), 20 ng/mL recombinant human basic fibroblast growth factor (Peprotech), and 20 ng/mL recombinant human epidermal growth factor (Peprotech). Cell cultures were fed with 1/3 volume of fresh medium every other day and passaged once per week via neurosphere dissociation. Cell cultures were maintained for 1 to 2 passages (roughly two weeks) after thawing prior to use in all *in vitro* and *in vivo* experiments.

Oligonucleotide delivery to GBM neurospheres *in vitro*

For efficacy studies, GBM8-fLuc cells were plated at 50,000 cells per well in 96-well tissue culture plates. Chol-hsiRNAs were diluted to twice the final concentration in OptiMEM (Gibco), and 50 μL diluted Chol-hsiRNA was added to 50 μL of cells and were subsequently incubated for 72 hours at 37°C and 5% CO_2. mRNA levels were quantified from cells using the QuantiGene 2.0 DNA Assay (Affymetrix) as described previously (18). Luciferase levels were quantified using a modified Dual-Glo Luciferase Assay System (Promega). Briefly, 50 μL of Dual-Glo Luciferase Assay Reagent was added to each well, incubated for 10 minutes, and luminescence was recorded on an Infinite M1000 Pro microplate reader (Tecan). For fluorescence imaging studies, GBM8-fLuc cells were plated at 100,000 cells/mL in 6-well tissue culture plates. Cells were counterstained with NucBlue Live Cell Stain ReadyProbes reagent (Life Technologies) according to the manufacturer's recommended protocol. Cy3-labeled Chol-hsiRNAs were added to the wells to a final concentration of 0 to 0.75 μmol/L and incubated for 0 to 5 hours at 37°C and 5% CO_2. Neurospheres were collected by centrifugation, affixed them to slides using a Shandon EZ Double Cytofunnel, fixed in 4% paraformaldehyde, and imaged on a Leica DMi8 inverted fluorescence microscope (40X oil objective). Intensity and exposure settings were the same for all samples. Images were processed using ImageJ (1.47v) software.

Tumor engraftment in mouse brain

Athymic nude female mice (6–8 weeks old) were used in all studies. The humane endpoint for xenografted mice was defined as the loss of >15% of maximum body weight or appearance of

any moribund symptoms (such as hunched posture). All animal procedures were approved by the University of Massachusetts Medical School Institutional Animal Care and Use Committee (protocol number A-2061).

On the day of surgery, GBM8-fLuc cells were dissociated and prepared as a single-cell suspension in sterile Dulbecco's PBS (Gibco). Animals were anesthetized, and 50,000 cells in 1 μL were injected by stereotactic placement into the right striatum (coordinates relative to bregma: +0.5 mm AP, −2.0 mm ML, and −2.5 mm DV from skull surface) at an infusion rate of 0.125 μL/min. The kinetics of tumor growth were monitored by *in vivo* imaging of tumor-associated bioluminescence signal using an IVIS 100 (Perkin-Elmer) as described (TABS; Supplementary Table S1; ref. 17). Data acquisition and quantification were performed using Living Image 4.2 software (Perkin-Elmer).

Oligonucleotide delivery to established xenografts in mouse brain

Tumor growth was monitored by *in vivo* bioluminescence imaging of tumor-associated luciferase activity (TABS) as described, and tumor-bearing mice assigned to groups with identical average TABS (17). Tumor-bearing athymic nude female mice (6–8 weeks old) were anesthetized and received stereotaxic injections of Chol-hsiRNAs into either the tumor (same coordinates used for tumor implantation) or the ipsilateral ventricle (coordinates relative to bregma: −0.2 mm AP, −0.8 mm ML, and −2.0 mm DV from skull surface).

For biodistribution studies, mice were injected intratumorally as described previously. Animals with roughly equivalent TABS (500,000 and 461,000 p/sec/cm^2/sr) were selected to evaluate the distribution of the fluorescently labeled Chol-hsiRNA within the tumor microenvironment (Supplementary Table S1). After 48 hours, mice were euthanized and perfused with PBS and 4% paraformaldehyde solution, and brains were postfixed in 2% paraformaldehyde for 48 hours. Paraffin 4 μm coronal brain sections through the striatum were stained with hematoxylin and eosin for neuropathological analysis and with DAPI for biodistribution analysis of Cy3-labeled Chol-hsiRNAs in tumors. Images were acquired on a Leica DMi8-inverted microscope (40X).

For intratumoral efficacy studies, animals ($n = 5$ per group) were injected with 2 μL of artificial cerebrospinal fluid (aCSF—120 mmol/L NaCl, 25 mmol/L $NaHCO_3$, 2.5 mmol/L KCl, 1 mmol/L NaH_2PO_4, 1.3 mmol/L $MgCl_2$, 10 mmol/L glucose), Chol-hsiRNA^{fLuc} (31–62 μg, 2.5–5 nmol), Chol-hsiRNA^{HTT} (62 μg, 5 nmol), or Chol-hsiRNA^{NTC} (62 μg, 5 nmol) at an infusion rate of 0.125 μL/min. For intracerebroventricular efficacy studies, animals ($n = 5$ per group) were injected with 5 μL of aCSF, Chol-hsiRNA^{fLuc} (31–62 μg, 2.5–5 nmol), or Chol-hsiRNA^{NTC} (62 μg, 5 nmol) at an infusion rate of 0.5 μL/min.

Oligonucleotide-mediated silencing of mRNA and protein *in vivo*

For efficacy studies, brains were collected 1 week after injection. Three 300 μm coronal sections through the striatum were collected, and from each section, a 2 mm punch was taken from the ipsilateral striatum and placed in RNAlater (Ambion) for 24 hours at 4°C. For mRNA quantification, each punch was lysed and processed as an individual sample for Quantigene 2.0 assay analysis (Affymetrix) and averaged for a single animal point (18). Luciferase activity in tissues was measured using the Promega Dual-Glo Luciferase Assay System, as described earlier (19), and normalized to total protein content measured by a Bradford assay.

Statistical analysis

Data were analyzed using GraphPad Prism 6 software (GraphPad Software, Inc.). For each independent mouse experiment, the level of mRNA silencing at each dose was normalized to the mean of the aCSF-injected control group. *In vivo* data were analyzed using a one-way ANOVA with a *post hoc* Bonferroni multiple comparisons test.

Results

Human primary glioma neurospheres productively internalize Chol-hsiRNAs *in vitro*

We evaluated the efficacy of Chol-hsiRNA (Fig. 1A) to silence gene expression in GBM. For these studies, we used GBM8, a well-validated GBM-initiating stem-like cell line that recapitulates the migratory and invasive properties of human GBM following implantation into the brain of immunocompromised mice (12, 20, 21). First, we assessed the activity of Chol-hsiRNAs toward GBM8 neurospheres *in vitro* (Supplementary Table S2). When added directly to the media, Chol-hsiRNAs were rapidly internalized by GBM8 neurospheres, over a period of hours (Fig. 1B). Chol-hsiRNA uptake is productive, as treatment of cells with hsiRNAs targeting *PPIB* mRNA (Cyclophilin B; PPIB-567) or *HTT* mRNA (Huntingtin; HTT-10150) for 72 hours reduced target mRNA levels by more than 90% (Fig. 1C) and 65%, respectively (Fig. 1D). No off-target silencing of either gene was observed following treatment with a nontargeting (scrambled) Chol-hsiRNA control (Chol-hsiRNA^{NTC}, Fig. 1C and D, gray bar, 3 μmol/L). This cell line was transduced with the lentivirus vector CSCW2-fLuc-IRES-mCherry to generate GBM8-fLuc cells that constitutively express firefly luciferase and mCherry protein (22). Using a *fLuc*-targeting Chol-hsiRNA (Chol-hsiRNA^{fLuc}), we assessed silencing of luciferase mRNA and protein at 72 hours after treatment. We observed an 82% reduction in luciferase mRNA (Fig. 2A) and a concomitant 90% reduction in luciferase activity (Fig. 2B). To ensure these effects were not due to compound toxicity, we assessed luciferase activity over a broad range of Chol-hsiRNA^{NTC} concentrations (0.1–6 μmol/L) and found no significant decrease in luciferase activity compared with the untreated control (Fig. 2C). We did not observe any significant reduction in GBM8 cell viability following administration of up to 5 μmol/L Chol-hsiRNA (Fig. S1, Supplementary Methods). In addition, we monitored neurosphere morphology at the highest doses of each compound (Fig. 2D; 3 μmol/L Chol-hsiRNA^{fLuc}; 6 μmol/L Chol-hsiRNA^{NTC}). There were no striking visual differences in neurosphere size (~250 μm) or number, suggesting that Chol-hsiRNA treatment did not trigger GBM8 cell death. Thus, Chol-hsiRNAs provide a simple and straightforward approach to achieve potent and specific mRNA silencing in GBM8 cells.

Chol-hsiRNA distributes throughout brain tumors after direct injection

We next interrogated the ability of Chol-hsiRNAs to distribute and silence gene expression in orthotopic GBM8 tumors in mouse brain. Two weeks after GBM8-fLuc tumor cell implantation, we

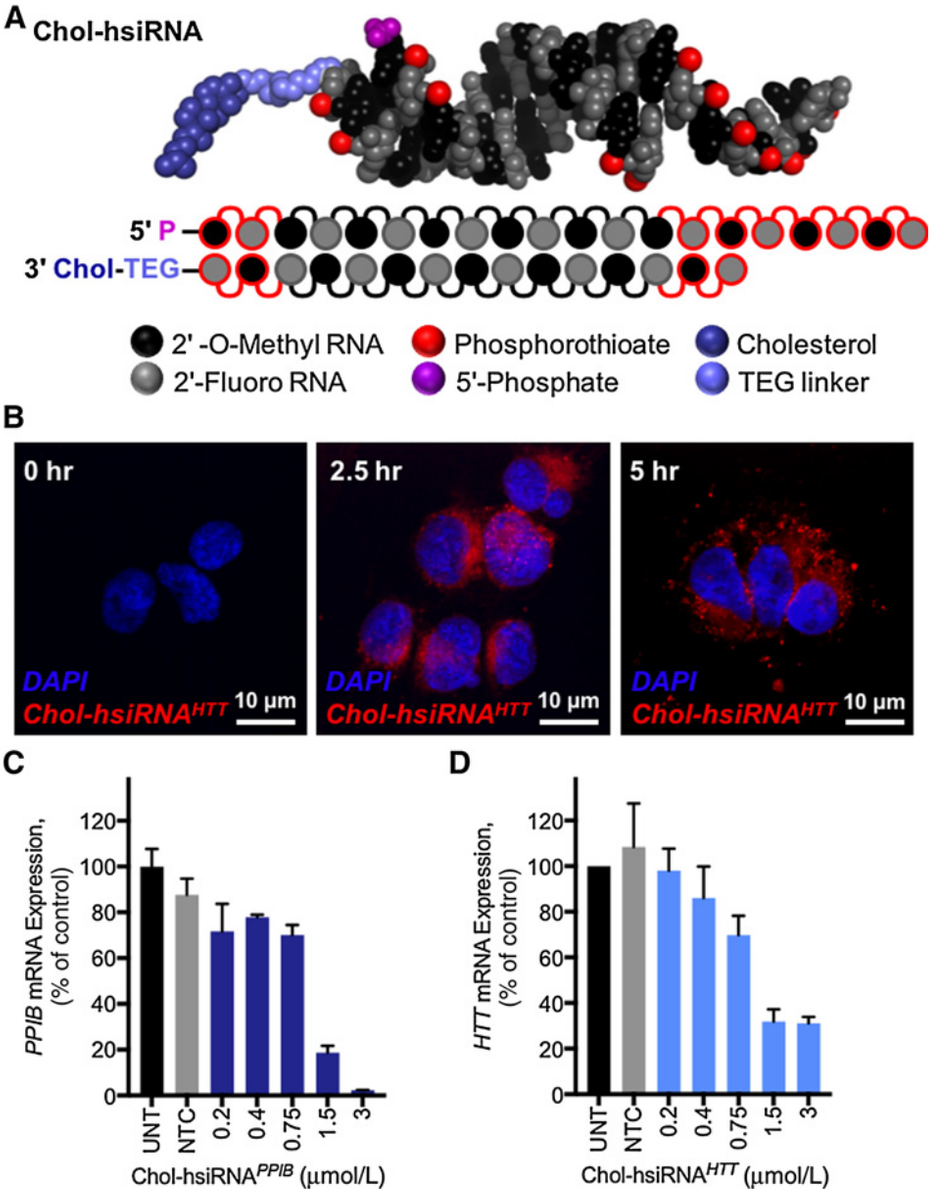

Figure 1.
Human primary GBM8 neurospheres productively internalize Chol-hsiRNA *in vitro*. **A,** Molecular model of a fully chemically modified, hydrophobic siRNA (Chol-hsiRNA) containing a cholesterol-tetraethyleneglycol (TEG) linker (blue) with 2′ fluoro (gray), 2′-O-methyl (black), phosphorothioate (red), and 5′-phosphate (purple) stabilizing modifications (PyMOL, Version 1.8, Schrödinger). **B,** Internalization kinetics into GBM8 neurospheres were assessed using 0.75 µmol/L Cy3-Chol-hsiRNA^{Htt} for 0 to 5 h. Nuclei (Hoechst), blue; Chol-hsiRNA (Cy3), red. Intensity and exposure settings were kept consistent between samples. Silencing of (**C**) *PPIB* and (**D**) *HTT* mRNA in GBM8 neurospheres following treatment with Chol-hsiRNA^{PPIB} or Chol-hsiRNA^{HTT}, respectively. *PPIB* and *HTT* mRNA levels were measured after 72 hours and normalized to a housekeeping gene (*HPRT*), and represented as percentage of untreated control ($n = 3$ biological replicates, mean ± SD). UNT, untreated cells; NTC, nontargeting (scrambled) Chol-hsiRNA control.

injected 5 nmol Cy3-labeled Chol-hsiRNA^{HTT} (5 nmol, 62.5 µg) into the tumor and analyzed distribution after 48 hours. As previously reported (17), GBM8-fLuc cells infiltrated the right hemisphere and exhibited characteristic hypercellular morphology with hyperchromatic nuclei, frequent mitoses, and necrosis (Fig. 3A). Cy3-labeled Chol-hsiRNA^{HTT} distributed broadly throughout the main tumor mass (Fig. 3B, dotted white line). At higher magnification, we observed Cy3-labeled Chol-hsiRNA^{HTT} accumulation in cytoplasmic foci, in addition to strong staining of the extracellular matrix and axonal bundles (Fig. 3B, arrows). This distribution pattern has been observed previously for Chol-hsiRNA following intraparenchymal injection into wild-type mouse striatum (11). We concluded that Chol-hsiRNAs distribute throughout established GBM8 tumors and are effectively taken up by tumor cells following a single, intratumoral injection.

Intratumoral injection of Chol-hsiRNA potently silences gene expression in brain tumors

Next, we analyzed the ability of Chol-hsiRNAs to silence gene expression in GBM8 tumors at 2 and 4 weeks after implantation. In these studies, we targeted two genes selectively expressed in the tumor (human *HTT* and *fLuc*), to distinguish from silencing in normal mouse brain cells. We first sought to determine whether intratumoral or intracerebroventricular injection was a superior route of administration to silence gene expression in established brain tumors. Tumor-bearing mice received either an intratumoral or intracerebroventricular injection of Chol-hsiRNA^{HTT} 4 weeks after tumor implantation. One week after injection, we observed a 45% reduction in human *HTT* following a 2 nmol intratumoral injection and a 23% reduction in human *HTT* following a 5 nmol ICV injection, compared with a control injected with aCSF (Fig. 4A).

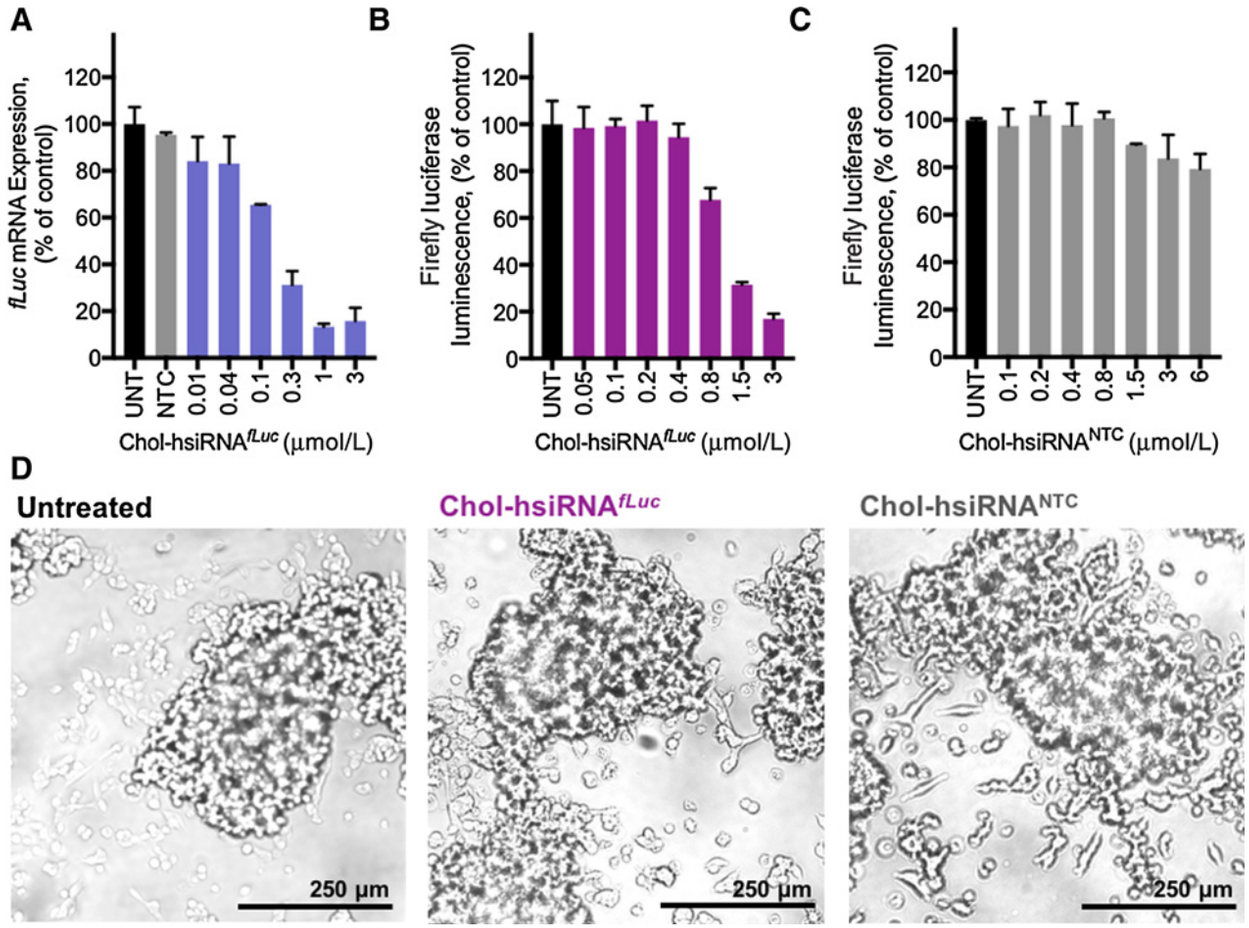

Figure 2.

Firefly luciferase–targeting Chol-hsiRNA silences *fLuc* mRNA and protein expression in GBM8 neurospheres. **A,** Human primary GBM8 cultures were incubated with Chol-hsiRNA^{fLuc} at concentrations shown, and *fLuc* mRNA levels were measured at 72 hours and normalized to the human housekeeping gene *PPIB*. *fLuc* mRNA levels are represented as percentage of untreated control ($n = 3$, mean ± SD). **B** and **C,** GBM8 cultures were incubated with (**B**) Chol-hsiRNA^{fLuc} or (**C**) Chol-hsiRNA^{NTC} at concentrations shown for 96 hours. Luciferase activity is represented as percentage of untreated control ($n = 3$ biological replicates, mean ± SD). UNT, untreated cells; NTC, nontargeting siRNA control. **D,** GBM8 neurospheres were monitored for number, size, and morphology following incubation with untreated medium, 3 μmol/L Chol-hsiRNA^{fLuc}, and 6 μmol/L Chol-hsiRNA^{NTC}. Representative images are shown.

As a single intratumoral injection achieved greater levels of mRNA silencing, we proceeded with that route of administration for the subsequent studies.

Next, we assessed protein silencing after intratumoral delivery of Chol-hsiRNA^{fLuc} to 2-week old GBM8-fLuc tumors. One week after intratumoral injection of either 2.5 or 5 nmol of Chol-hsiRNA^{fLuc}, we observed an approximately 90% reduction in luciferase activity relative to the aCSF-injected control (Fig. 4B). The heterogeneity in luciferase activity for the Chol-hsiRNA^{NTC}-injected animals is likely due to variability in tumor size at the 2-week time point. Taken together, these data suggest that the Chol-hsiRNAs chemical architecture is an effective platform to silence gene expression in brain tumors *in vivo* by direct intratumoral administration.

Discussion

GBM tumors are highly heterogeneous cellular ecosystems, composed of self-renewing stem-like cells (GSCs), differentiated cells, nonmalignant brain cells, and immune cells (23). GSCs are emerging as key effectors in tumor malignancy, resistance, and reoccurrence. Therapeutic targeting of GSCs represents one of the most direct routes toward curbing GBM tumorigenesis. The outstanding challenges in targeting GSCs are identifying a therapeutic platform that is capable of modulating expression or activity of GBM driver genes and achieving targeted GSC delivery. Genome sequencing and transcriptomic and epigenetic profiling have unveiled gene clusters altered or misregulated in GBM, including aberrant methylation sites, histone modification patterns, and chromatin architectures (23, 24). The vast majority of these targets are undruggable by conventional small molecule and biologics approaches (10). Oligonucleotides are powerful tools for precise, multi-target gene silencing in the central nervous system (11, 15, 25), as both potential therapeutics and methods of probing the functional genomics of GBM (26). However, delivery is the key obstacle preventing immediate deployment of siRNAs against the molecular drivers of GBM.

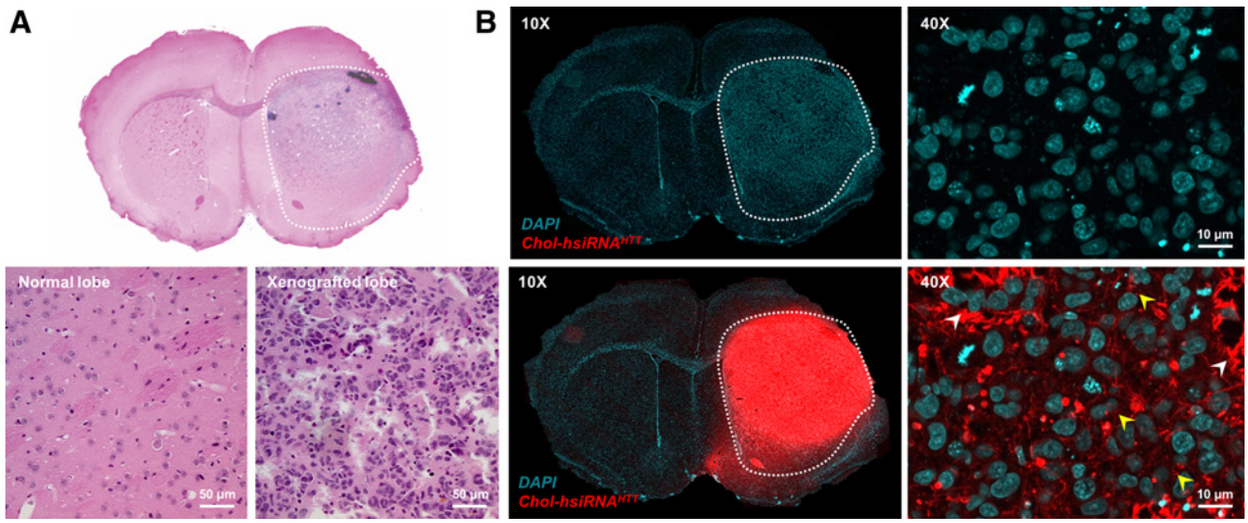

Figure 3.
Chol-hsiRNA distributes evenly throughout the brain tumor xenograft after intratumoral injection. Cy3-labeled Chol-hsiRNA^{HTT} was injected into established orthotopic GBM8 brain tumors. Distribution was analyzed at 24 hours after injection. **A,** Tiled (10X) and magnified (20X) coronal images of hematoxylin and eosin (H&E) staining delineating tumor border in xenografted lobe. **B,** Tiled (10X) and magnified (40X) fluorescence images of coronal brain sections imaged for nuclear (DAPI, blue) and Chol-hsiRNA (Cy3, red) signal. White arrows indicate Chol-hsiRNA aggregation with axonal bundles. Yellow arrows indicate Chol-hsiRNA accumulation in cytoplasmic foci. Representative images, confirmed in two separate experiments.

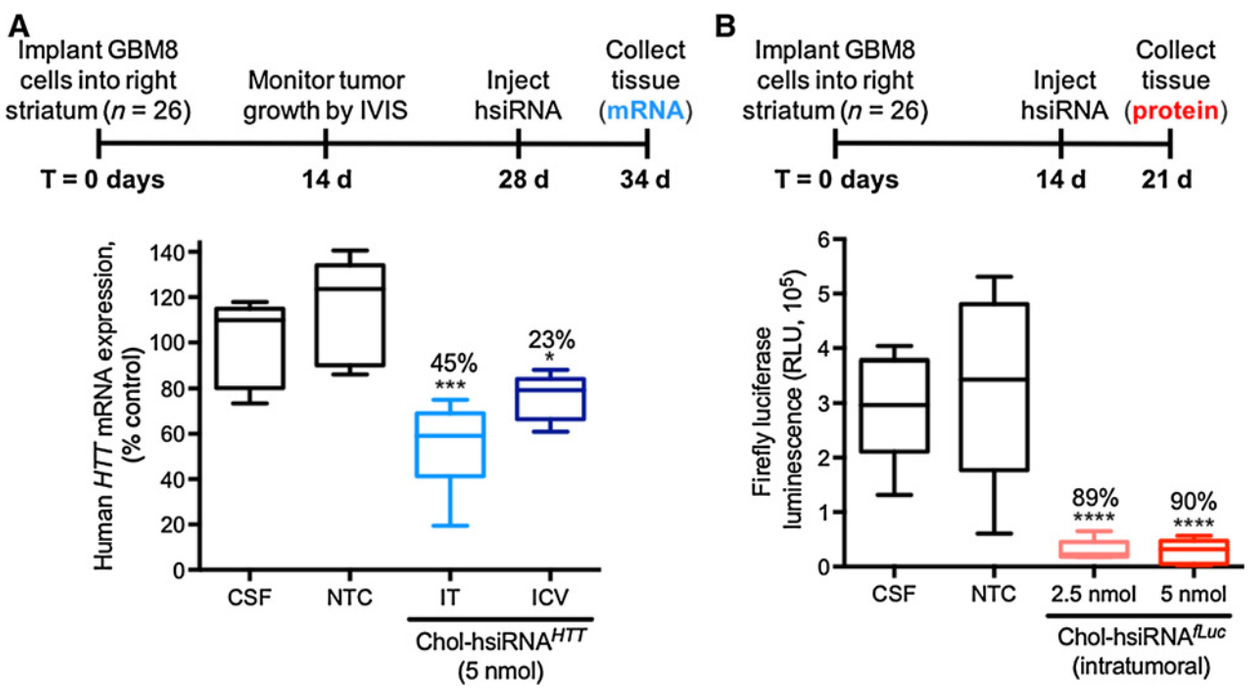

Figure 4.
Chol-hsiRNA silences human *HTT* mRNA and firefly luciferase protein expression in brain tumors after direct injection. **A,** Changes in human *HTT* mRNA levels 1 week after intratumoral injection of aCSF, 5 nmol of nontargeting control Chol-hsiRNA^{NTC} (NTC), 5 nmol Chol-hsiRNA^{HTT}, or ICV injection of 5 nmol Chol-hsiRNA^{HTT} into 4-week-old GBM8 tumors. Data were normalized for the human housekeeping gene *PPIB* and represented as a percentage of untreated control ($n = 5$ mice, mean ± SD, three biopsies per striatum). **B,** Changes in tumor-associated luciferase activity 1 week after intratumoral injection of Chol-hsiRNA^{fLuc} (2.5 or 5 nmol) or Chol-hsiRNA^{NTC} (5 nmol) in 2-week-old GBM8 tumors ($n = 5$ mice, mean ± SD, three biopsies per striatum). Percentages reflect degree of luminescence reduction (*, $P < 0.05$; **, $P < 0.01$; ***, $P < 0.001$; and ****, $P < 0.0001$).

The two primary approaches to achieve synthetic siRNA delivery are through formulations or direct conjugation (27). siRNA formulations or encapsulations (e.g., lipid nanoparticles) that are typically used to improve stability and retention in other organs show pronounced neuroinflammation and neuronal toxicity in brain (28–30). Direct lipid conjugation holds great promise to achieve safe, carrier-free siRNA delivery for neurological applications (11, 15, 25). Previously, we described the pharmacokinetic properties of cholesterol-conjugated hsiRNAs in mouse brain, demonstrating that Chol-hsiRNAs were rapidly internalized into neurons and glia, inducing potent gene silencing after an intraparenchymal injection in mouse striatum (11). Due to their lipophilicity, Chol-hsiRNAs were retained around the site of injection, exhibiting highly efficient cellular internalization (11). These considerations prompted us to investigate Chol-hsiRNAs as a platform for localized RNAi-mediated gene silencing in GSC-derived established tumors.

In the current report, we demonstrate that Chol-hsiRNAs are rapidly internalized into patient-derived GBM8 neurospheres, inducing significant mRNA and protein silencing *in vitro* with no observable toxicity. We show that Chol-hsiRNAs distribute broadly throughout established GBM8 brain tumors, inducing potent (>90%) and durable (7 days) silencing of tumor-specific reporter genes. This comprises the first report of efficient gene silencing in a GSC-derived orthotopic brain tumor by a lipid-conjugated siRNA. Chol-hsiRNAs have predictable pharmacokinetic properties and can be used to target single genes, or used in combination to modulate entire networks (9). Moreover, the low dosing requirements afforded by chemically modified siRNAs with enhanced stability and efficiency minimize the risk of off-target effects, collateral damage to healthy tissues, and unintended systemic toxicity (9). For instance, the most clinically advanced siRNA (a fully 2′ substituted, trivalent N-acetylgalactosamine-siRNA conjugate) achieved over 6 months of sustained target silencing in patients after a single dose, with no serious adverse events (31).

Recent key studies have validated multiplexed siRNA therapies as a strategy for improving survival in GSC tumor models (10) and have demonstrated the potential for unformulated oligonucleotides to effectively penetrate the blood–tumor barrier at high doses (20, 32). We continue to investigate the ability of other classes of lipid-conjugated siRNAs to achieve potent gene silencing in brain tumors through systemic or CSF delivery. Polyunsaturated fatty acid-siRNAs exemplify a new class of conjugates we are exploring for gene silencing in CNS (15, 25). Last year witnessed the clinical approval of Spinraza (nusinersen), a splice-switching antisense oligonucleotide for the treatment of spinal muscular atrophy (33). The rapid evolution of oligonucleotide chemistries will soon yield entities capable of translation into potent new GBM therapies, based on our expanding knowledge of the genetic changes that drive the biogenesis and growth of these devastating tumors.

Disclosure of Potential Conflicts of Interest

D. Golebiowski is Senior Research Scientist at Solid Biosciences. A. Khvorova has ownership interest (including patents) in the stocks of RXi Pharmaceuticals and Advirna, LLC. No potential conflicts of interest were disclosed by the other authors.

Authors' Contributions

Conception and design: M.F. Osborn, A.H. Coles, D. Golebiowski, M. Sena-Esteves, A. Khvorova

Development of methodology: M.F. Osborn, A.H. Coles, D. Golebiowski, D. Echeverria

Acquisition of data (provided animals, acquired and managed patients, provided facilities, etc.): M.F. Osborn, A.H. Coles, D. Golebiowski

Analysis and interpretation of data (e.g., statistical analysis, biostatistics, computational analysis): M.F. Osborn, A.H. Coles, M.P. Moazami, M. Sena-Esteves, A. Khvorova

Writing, review, and/or revision of the manuscript: M.F. Osborn, A.H. Coles, D. Golebiowski, J.K. Watts, M. Sena-Esteves, A. Khvorova

Administrative, technical, or material support (i.e., reporting or organizing data, constructing databases): M.F. Osborn, D. Golebiowski, A. Khvorova

Study supervision: M.F. Osborn, J.K. Watts, M. Sena-Esteves, A. Khvorova

Acknowledgments

We gratefully acknowledge funding from NIH S10 OD020012 (to A. Khvorova), NIH R01 GM108803-02 (to A. Khvorova), and NIH F32 NS095508-02 (to M.F. Osborn).

The costs of publication of this article were defrayed in part by the payment of page charges. This article must therefore be hereby marked *advertisement* in accordance with 18 U.S.C. Section 1734 solely to indicate this fact.

Received November 16, 2017; revised February 1, 2018; accepted April 3, 2018; published first April 13, 2018.

References

1. Wen PY, Reardon DA. Neuro-oncology in 2015: progress in glioma diagnosis, classification and treatment. Nat Rev Neurol 2016;12:69–70.
2. Lozada-Delgado EL, Grafals-Ruiz N, Vivas-Mejia PE. RNA interference for glioblastoma therapy: innovation ladder from the bench to clinical trials. Life Sci 2017;188:26–36.
3. Van Meir EG, Hadjipanayis CG, Norden AD, Shu HK, Wen PY, Olson JJ. Exciting new advances in neuro-oncology: the avenue to a cure for malignant glioma. CA Cancer J Clin 2010;60:166–93.
4. Alifieris C, Trafalis DT. Glioblastoma multiforme: pathogenesis and treatment. Pharmacol Ther 2015;152:63–82.
5. Ellis HP, Greenslade M, Powell B, Spiteri I, Sottoriva A, Kurian KM. Current challenges in glioblastoma: intratumour heterogeneity, residual disease, and models to predict disease recurrence. Front Oncol 2015;5:251.
6. Seymour T, Nowak A, Kakulas F. Targeting aggressive cancer stem cells in glioblastoma. Front Oncol 2015;5:159.
7. Lathia JD, Mack SC, Mulkearns-Hubert EE, Valentim CL, Rich JN. Cancer stem cells in glioblastoma. Genes Dev 2015;29:1203–17.
8. Hopkins AL, Groom CR. The druggable genome. Nat Rev Drug Discov 2002;1:727–30.
9. Khvorova A, Watts JK. The chemical evolution of oligonucleotide therapies of clinical utility. Nat Biotechnol 2017;35:238–48.
10. Yu D, Khan OF, Suva ML, Dong B, Panek WK, Xiao T, et al. Multiplexed RNAi therapy against brain tumor-initiating cells via lipopolymeric nanoparticle infusion delays glioblastoma progression. Proc Natl Acad Sci U S A 2017;114:E6147–E56.
11. Alterman JF, Hall LM, Coles AH, Hassler MR, Didiot MC, Chase K, et al. Hydrophobically modified siRNAs silence huntingtin mRNA in primary neurons and mouse brain. Mol Ther Nucleic Acids 2015;4:e266.
12. Wakimoto H, Kesari S, Farrell CJ, Curry WT Jr, Zaupa C, Aghi M, et al. Human glioblastoma-derived cancer stem cells: establishment of invasive glioma models and treatment with oncolytic herpes simplex virus vectors. Cancer Res 2009;69:3472–81.
13. Byrne M, Tzekov R, Wang Y, Rodgers A, Cardia J, Ford G, et al. Novel hydrophobically modified asymmetric RNAi compounds (sd-rxRNA) demonstrate robust efficacy in the eye. J Ocul Pharmacol Ther 2013;29:855–64.
14. Allerson CR, Sioufi N, Jarres R, Prakash TP, Naik N, Berdeja A, et al. Fully 2′-modified oligonucleotide duplexes with improved in vitro potency and

stability compared to unmodified small interfering RNA. J Med Chem 2005;48:901–4.
15. Nikan M, Osborn MF, Coles AH, Godinho BM, Hall LM, Haraszti RA, et al. Docosahexaenoic acid conjugation enhances distribution and safety of siRNA upon local administration in mouse brain. Mol Ther Nucleic Acids 2016;5:e344.
16. Huang Y. Preclinical and clinical advances of GalNAc-decorated nucleic acid therapeutics. Mol Ther Nucleic Acids 2017;6:116–32.
17. GuhaSarkar D, Neiswender J, Su Q, Gao G, Sena-Esteves M. Intracranial AAV-IFN-beta gene therapy eliminates invasive xenograft glioblastoma and improves survival in orthotopic syngeneic murine model. Mol Oncol 2017; 11:180–93.
18. Coles AH, Osborn MF, Alterman JF, Turanov AA, Godinho BM, Kennington L, et al. A high-throughput method for direct detection of therapeutic oligonucleotide-induced gene silencing in vivo. Nucleic Acid Ther 2016; 26:86–92.
19. Osborn MF, Alterman JF, Nikan M, Cao H, Didiot MC, Hassler MR, et al. Guanabenz (Wytensin) selectively enhances uptake and efficacy of hydrophobically modified siRNAs. Nucleic Acids Res 2015;43:8664–72.
20. Teplyuk NM, Uhlmann EJ, Gabriely G, Volfovsky N, Wang Y, Teng J, et al. Therapeutic potential of targeting microRNA-10b in established intracranial glioblastoma: first steps toward the clinic. EMBO Mol Med 2016; 8:268–87.
21. Ledur PF, Onzi GR, Zong H, Lenz G. Culture conditions defining glioblastoma cells behavior: what is the impact for novel discoveries? Oncotarget 2017;8:69185–97.
22. GuhaSarkar D, Su Q, Gao G, Sena-Esteves M. Systemic AAV9-IFNbeta gene delivery treats highly invasive glioblastoma. Neuro Oncol 2016;18: 1508–18.
23. Patel AP, Tirosh I, Trombetta JJ, Shalek AK, Gillespie SM, Wakimoto H, et al. Single-cell RNA-seq highlights intratumoral heterogeneity in primary glioblastoma. Science 2014;344:1396–401.
24. Zorzan M, Giordan E, Redaelli M, Caretta A, Mucignat-Caretta C. Molecular targets in glioblastoma. Future Oncol 2015;11:1407–20.
25. Nikan M, Osborn MF, Coles AH, Biscans A, Godinho B, Haraszti RA, et al. Synthesis and evaluation of parenchymal retention and efficacy of a metabolically stable O-phosphocholine-N-docosahexaenoyl-l-serine siRNA conjugate in mouse brain. Bioconjug Chem 2017;28:1758–66.
26. Dudley A, Sater M, Le PU, Trinh G, Sadr MS, Bergeron J, et al. DRR regulates AKT activation to drive brain cancer invasion. Oncogene 2014;33: 4952–60.
27. Juliano RL. The delivery of therapeutic oligonucleotides. Nucleic Acids Res 2016;44:6518–48.
28. Zhang Y, Zhang YF, Bryant J, Charles A, Boado RJ, Pardridge WM. Intravenous RNA interference gene therapy targeting the human epidermal growth factor receptor prolongs survival in intracranial brain cancer. Clin Cancer Res 2004;10:3667–77.
29. Krichevsky AM, Kosik KS. RNAi functions in cultured mammalian neurons. Proc Natl Acad Sci U S A 2002;99:11926–9.
30. Mathupala SP. Delivery of small-interfering RNA (siRNA) to the brain. Expert Opin Ther Pat 2009;19:137–40.
31. Fitzgerald K, Kallend D, Simon A. A highly durable RNAi therapeutic inhibitor of PCSK9. N Engl J Med 2017;376:e38.
32. Lee TJ, Haque F, Shu D, Yoo JY, Li H, Yokel RA, et al. RNA nanoparticle as a vector for targeted siRNA delivery into glioblastoma mouse model. Oncotarget 2015;6:14766–76.
33. Wadman M. Antisense rescues babies from killer disease. Science 2016; 354:1359–60.